# Non-unity Permeability in InP-based Mach-Zehnder Interferometer with Metamaterial

Tomohiro Amemiya[1,2], Takahiko Shindo[2], Seiji Myoga[2], Nobuhiko Nishiyama[2], and Shigehisa Arai[1,2]
[1]Quantum Nanoelectronics Research Center, [2]Dpartment of Electrical and Electronic Engineering
Tokyo Institute of Technology, 2-12-1-S9-5 O-okayama, Meguro-ku, Tokyo 152-8552, Japan
amemiya.t.ab@m.titech.ac.jp, arai@pe.titech.ac.jp

***Abstract*—An InP-based Mach-Zehnder interferometer combined with a metamaterial layer consisting of a split-ring resonator array was realized for observing phase shift due to the metamaterial effect. At 1.5-μm wavelength, the metamaterial showed non-unity relative permeability induced by magnetic interaction with propagating light in the device.**

## I. Introduction

Controlling the permeability of semiconductors used in photonic devices is one of innovative means to open a new field in optical communication technology. A promising method of permeability control is to make use of the concept of metamaterials that can materialize 'non-unity' relative permeability ($\mu \neq 1$) at optical frequencies. Several photonic applications based on metamaterials have been proposed; leading examples are the glass-based trapped rainbow storage of light [1] and the fiber-based metamaterial light source [2].

It is a promising challenge to introduce metamaterials into InP-based waveguide devices such as lasers, modulators, and optical switches. For this purpose, we have developed GaInAsP/InP multimode-interferometers (MMIs) and related devices combined with split-ring resonator (SRR) arrays that operate as a metamaterial [3, 4]. At 1.5-μm wavelength, the non-unity permeability was confirmed in the device, which was induced by magnetic interaction between the SRRs and light propagating in the MMI waveguide.

To use the SRR array as a metamaterial, it is important to know its effective permeability accurately. However, accurate permeability data cannot be extracted from the simple transmission data of the previous devices because the transmission data also includes the effect of SRR's effective permittivity. To cope with this problem, we have proposed a measurement method that uses a Mach-Zehnder interferometer (MZI) and successfully obtained the accurate permeability value for the SRR array. The following provides the outline of our results.

## II. Principle and Fabrication

Our MZI device is shown in Fig. 1. It consists of two 3-dB couplers and two arms made with GaInAsP/InP ridge waveguides, with a metal SRR array attached on one of the arms. For TE-mode input light with the SRR-resonance frequency, the SRR array interacts with the light, thereby behaving as a material with a complex refractive-index. The real part of the refractive-index affects the phase of traveling light, thereby changing the phase difference at the output coupler. The imaginary part causes the propagation loss of light in the arm. The transmittance of the MZI is determined by the phase difference and propagation loss.

The propagation loss in the arms can be inferred from the transmission data of straight waveguides with/without the SRR array. Therefore, the effective permeability and permittivity of the SRR array can be calculated, using measured data for the transmittance of the MZI.

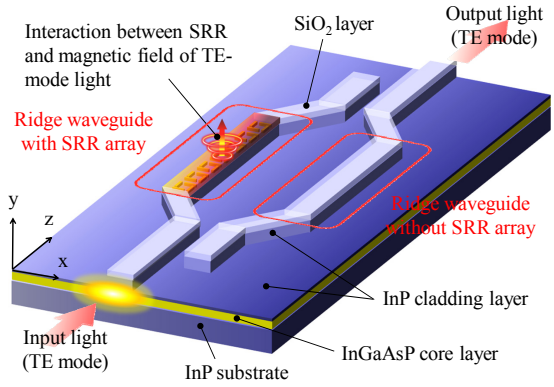


Fig. 1. Mach-Zehnder Interferometer consisting of GaInAsP/InP waveguides and metamaterial layer (SRR array) attached on one arm.

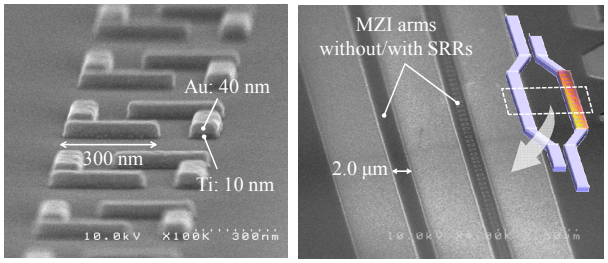


(a) (b)

Fig. 2. SRRs and arms of MZI: (a) oblique view of 4-cut SRRs, and (b) two arms, observed with SEM. One arm has a SRR array.

An actual MZI was made for measurement at 1.5-μm optical communication wavelength. Epitaxial layer structures were the same as those of our previous device [4]. On the surface of the device, an SRR array (consisting of 10-nm thick Ti and 40-nm thick Au) was formed using electron-beam lithography (EBL) and a lift-off process. Figure 2(a) shows the oblique images of the SRR array observed with a scanning electron microscope (SEM). The *4-cut* SRR was used because it has a high resonant frequency owing to its small gap capacitance [5]. The size of the SRR was designed for use at 1.5-μm band frequency (193 THz).

After the formation of the SRR array, a $SiO_2$ mask (100-nm thick) for the MZI pattern was formed on the device with plasma-enhanced chemical-vapor-deposition and EBL. With the $SiO_2$ mask, the MZI structure was formed using $CH_4/H_2$ reactive ion etching. Figure 2(b) shows the SEM image of the arms with/without the SRR array. The length of the SRR array along the arm was set to 500 μm. In addition to these experimental samples, straight ridge waveguides with/without the SRRs were

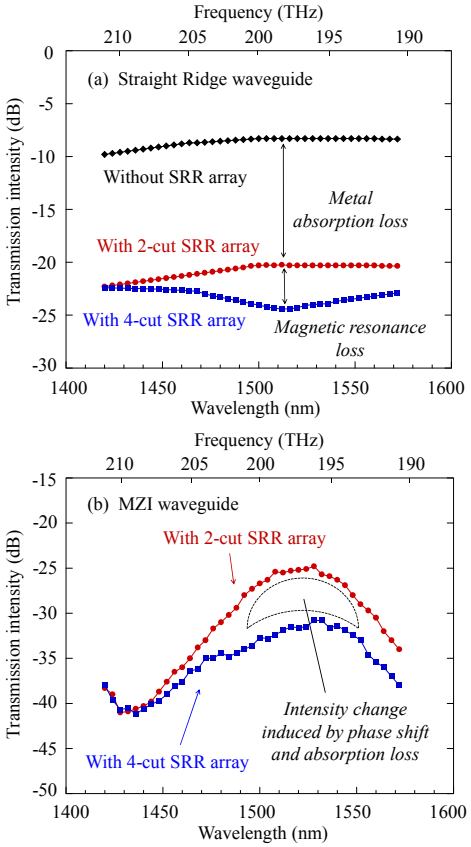


Fig. 3. Output intensity from devices with 4-cut SRRs (blue lines), 2-cut SRRs (res lines) and without SRRs (black lines) as a function of wavelength, measured for (a) straight ridge waveguides and (b) MZIs.

made. We also prepared control samples with SRRs consisting of *2-cut* square rings with the same size as that of the *4-cut* SRR. The *2-cut* SRR has a resonant frequency far higher than 193 THz, so it has no interaction with 1.5-μm light.

## III. Measurement Results and Discussion

In measurement, the input light was sent from a tunable laser to the devices through a polarization controller; its wavelength was changed in the range of 1420–1575 nm. The intensities of the output light from the device as a function of wavelength are shown in Figs. 3(a) and 3(b).

Figure 3(a) shows the output intensity for straight waveguides with 4-cut SRR array (blue dots), without SRRs (black dots), and with 2-cut SRRs (red dots). The difference between the curves without SRRs and that with 2-cut SRRs corresponds to a loss caused by light absorption of the SRR metal. The difference between the 2-cut SRRs and 4-cut SRRs shows the loss caused by the magnetic interaction between the SRRs and light. The 4-cut SRRs resonated at about 1510-1520 nm and showed the maximum loss at this wavelength.

Figure 3(b) shows the output intensity for MZIs with 4-cut SRRs and that for without SRRs. Their difference shows the intensity change induced by the phase shift and the absorption loss of light in the MZI. That is, the difference shows an intrinsic change in transmission intensity induced by the SRR resonance without including parasitic factors such as metal

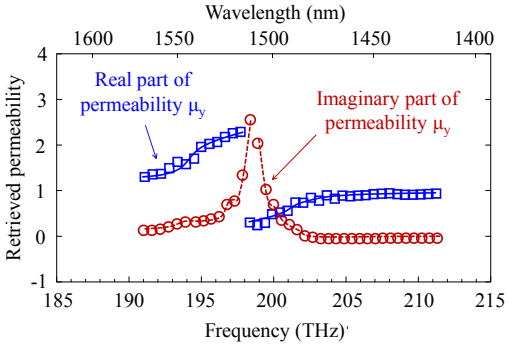


Fig. 4. Retrieved effective permeability (real and imaginary parts) of SRR array on MZI waveguide, plotted as a function of frequency.

absorption loss in the SRRs and lensed-fiber coupling loss in the measurement system.

On simple condition that the electric and magnetic fields are constant in the *x*-direction, that is, $\partial_x = 0$, the transfer matrix in each layer is given by

$$\mathrm{M}_m = \begin{pmatrix} \cosh(\beta_m d_m) & (j\omega\mu_0\mu_{zm}/\beta_m)\sinh(\beta_m d_m) \\ (\beta_m/j\omega\mu_0\mu_{zm})\sinh(\beta_m d_m) & \cosh(\beta_m d_m) \end{pmatrix},$$
$$\beta_m = \sqrt{(\mu_{zm}/\mu_{ym})\beta^2 - k_0^2\varepsilon_{xm}\mu_{zm}}, \quad (1)$$

where $\varepsilon_{xm}$, $\mu_{ym}$ and $\mu_{zm}$ are the diagonal elements of the permittivity and permeability tensor of the *m*-th layer, and $k_0$ is the free-space propagation constant. The permittivity $\varepsilon_x$ of the SRR array was calculated first, using the eigenvalue equation with Eq. (1) and the transmission intensity ratio (= (without SRRs)/(with 2-cut SRRs)) for the straight waveguides (see Fig. 3(a)). After that, the real and imaginary parts of permeability $\mu_y$ of the SRR array was retrieved, using the permittivity $\varepsilon_x$ and the transmission intensity ratio (= (2-cut SRRs)/(4-cut SRRs)) for the straight waveguide and that for the MZI. In calculation, the effective thickness $d_m$ of the SRR layer was set to 350 nm.

Figure 4 shows the retrieved permeability (real and imaginary parts) of the SRR array as a function of frequency. The permeability exhibited a resonance at 200 THz, and the real part of the relative permeability changed from +2.2 to -0.3 in the vicinity of this frequency. This results show the feasibility of semiconductor-based photonic devices combined with metamaterials.


## Acknowledgment

This research was financially supported by the Ministry of Education, Culture, Sports, Science and Technology (MEXT), Japan and the Japan Sciety for the Promotion of Science (JSPS) under Grants-in-Aid for Scientific Research (#19002009, #22360138, #21226010, #23760305, #10J08973) .


## References


[1] K. L. Tsakmakidis, A. D. Boardman, and O. Hess, "Trapped rainbow storage of light in metamaterials," *Nature*, Vol. 450, pp. 397-401, 2007.

[2] G. Adamo, K. F. MacDonald, F. De Angelis, E. Di Fabrizio, N. I. Zheludev, "Nanoscale electron-beam-driven metamaterial light sources," Proc. IEEE Photonics Society 23rd Annual Meeting, pp. 443-444, 2010.

[3] T. Amemiya, T. Shindo, D. Takahashi, N. Nishiyama, and S. Arai, "Magnetic Interactions at Optical Frequencies in InP-based Waveguide Device with Metamaterial," J. Quantum Electron. Vol. 47, No. 5, pp. 736-744, 2011.

[4] T. Amemiya, T. Shindo, D. Takahashi, S. Myoga, N. Nishiyama, and S. Arai, "Non-unity permeability in metamaterial-based GaInAsP/InP multimode interferometers," Optics Lett. Vol. 36, No. 12, pp. 2327-2329, 2011.

[5] A. Ishikawa, T. Tanaka, and S. Kawata, "Frequency dependence of the magnetic response of split-ring resonators," *J. Opt. Soc. Am. B*, vol. 24, no. 3, pp. 510–515, Mar. 2007.